

Formation and Dynamic Properties of the Triangular Rhodium μ_3 -Sulfido Complex $[\text{Rh}_3\text{Cp}^*_3(\mu_3\text{-}\eta^2\text{-}|\text{-C}_2\text{H}_2)(\mu_3\text{-S})]^{2+}$ ($\text{Cp}^* = \eta^5\text{-C}_5\text{Me}_5$), Including an Acetylene Ligand Generated by the Coupling and Deprotonation of Two Bridging Methylene Units in a Dirhodium Complex

Takanori Nishioka,[†] Kiyoshi Isobe,[‡] and Isamu Kinoshita[§]

Department of Material Science, Osaka City University, Sumiyoshi-ku, Osaka 558, Japan

Yoshiki Ozawa

Department of Material Science, Himeji Institute of Technology, Harima Science Park City, Hyogo 678-12, Japan

Amelio Vázquez de Miguel

Departamento de Química Inorgánica, Universidad de Alcalá de Henares, 28871 Alcalá de Henares, Madrid, Spain

Toshihito Nakai and Seiichi Miyajima

Institute for Molecular Science, Myodaiji, Okazaki 444, Japan

Received September 9, 1997

Summary: Deprotonation of the double-bridging $\mu_2\text{-CH}_2$ complex $[\text{Rh}_2\text{Cp}^*_2(\mu_2\text{-CH}_2)_2(\mu_2\text{-SH})](\text{BPh}_4)$ ($\text{Cp}^* = \eta^5\text{-C}_5\text{Me}_5$) with $[\text{Rh}_2\text{Cp}^*_2(\mu_2\text{-OH})_3](\text{BPh}_4)$ led to the isolation of the trirhodium $\mu_3\text{-S}$ complex $[\text{Rh}_3\text{Cp}^*_3(\mu_3\text{-}\eta^2\text{-}|\text{-C}_2\text{H}_2)(\mu_3\text{-S})](\text{BPh}_4)_2$, including an acetylene ligand generated by a unique C–C bond coupling and deprotonation of two $\mu_2\text{-CH}_2$ groups. The dynamic property of the acetylene complex in both solution and the solid state was studied by variable-temperature ^1H , ^{13}C , and CP/MAS ^{13}C NMR spectroscopy.

The coupling of bridging methylene species is an important step in solid surface reactions for producing hydrocarbons from CO and syngas.¹ The C–C bond coupling of two $\mu_2\text{-CH}_2$ ligands in doubly bridging methylene rhodium and ruthenium complexes takes place to form alkenes.^{1a,c,e,2} However, there has been no observation of the generation of alkynes in these coupling reactions.

Upon deprotonation of the $\mu_2\text{-SH}$ group in $[\text{Rh}_2\text{Cp}^*_2(\mu_2\text{-CH}_2)_2(\mu_2\text{-SH})](\text{BPh}_4)$ (**1**)³ with $[\text{Rh}_2\text{Cp}^*_2(\mu_2\text{-OH})_3](\text{BPh}_4)$ (**2a**)⁴ to synthesize a trirhodium $\mu_3\text{-S}$ complex, we have found an unexpected and unprecedented C–C bond coupling to form the acetylene ligand from two $\mu_2\text{-CH}_2$ groups with the creation of the novel $\mu_3\text{-S}$ trinuclear cluster $[\text{Rh}_3\text{Cp}^*_3(\mu_3\text{-}\eta^2\text{-}|\text{-C}_2\text{H}_2)(\mu_3\text{-S})]\text{X}_2$ (X = BPh₄ (**3a**), BF₄ (**3b**)). Here we report the formation of complex **3** involving a new C–C bond coupling and its dynamic behavior.

Complex **1**, $[\text{Rh}_2\text{Cp}^*_2(\mu_2\text{-CH}_2)_2(\mu_2\text{-SH})](\text{BPh}_4)$, has three characteristic functionalities of the Rh($\mu\text{-SH}$)Rh group: the Rh–Rh single bond and two $\mu_2\text{-CH}_2$ groups. By primarily using the Rh($\mu\text{-SH}$)Rh functionality, we have discovered its unique reactivities toward electrophiles such as O₂,⁵ Ag⁺,⁶ and unsaturated hydrocarbons.⁷ We now use all three functionalities of **1** to synthesize complex **3**. The reaction of $[\text{Rh}_2\text{Cp}^*_2(\mu_2\text{-CH}_2)_2(\mu_2\text{-SH})](\text{BPh}_4)$ (**1**) with $[\text{Rh}_2\text{Cp}^*_2(\mu_2\text{-OH})_3](\text{BPh}_4)$ (**2a**) in acetone at room temperature led to the formation of a trirhodium $\mu_3\text{-S}$ complex with an acetylene ligand, $[\text{Rh}_3\text{Cp}^*_3(\mu_3\text{-}\eta^2\text{-}|\text{-C}_2\text{H}_2)(\mu_3\text{-S})](\text{BPh}_4)_2$ (**3a**), in a 34% yield based on Rh.⁸ The BF₄ salt of **3b** was obtained from **3a** by anion exchange using Ph₄PBF₄. The mixed-metal

[†] E-mail: nishioka@sci.osaka-cu.ac.jp.

[‡] E-mail: isobe@sci.osaka-cu.ac.jp.

[§] E-mail: isamu@sci.osaka-cu.ac.jp.

(1) (a) Maitlis, P. M. *J. Organomet. Chem.* **1995**, *500*, 239 and references therein. (b) Maitlis, P. M. *Chem. Eng. News* **1996**, *74* (Aug 12) 31. (c) Maitlis, P. M.; Long, H. C.; Quyoum, R.; Turner, M. L.; Wang, Z.-Q. *J. Chem. Soc., Chem. Commun.* **1996**, *1*. (d) Akita, M.; Hua, R.; Oku, T.; Moro-oka, Y. *Organometallics* **1996**, *15*, 2548 and references therein. (e) Akita, M.; Hua, R.; Oku, T.; Tanaka, M.; Moro-oka, Y. *Organometallics* **1996**, *15*, 2548 and references therein. (f) Akita, M.; Hua, R.; Knox, S. A. R.; Moro-oka, Y.; Nakanishi, S.; Yates, M. I. *J. Chem. Soc., Chem. Commun.* **1997**, *51*.

(2) (a) Nutton, A.; Vázquez de Miguel, A.; Isobe, K.; Maitlis, P. M. *J. Chem. Soc., Chem. Commun.* **1983**, *166*. (b) Saez, I. M.; Meanwell, N. J.; Nutton, A.; Isobe, K.; Vázquez de Miguel, A.; Bruce, D. W.; Okeya, S.; Andrews, D. G.; Ashton, P. R.; Johnstone, I. R.; Maitlis, P. M. *J. Chem. Soc., Dalton Trans.* **1986**, *1565*. (c) Wang, Z.-Q.; Long, H. C.; Turner, M. L.; Maitlis, P. M. *J. Chem. Soc., Chem. Commun.* **1995**, *1089*.

(3) Ozawa, Y.; Vázquez de Miguel, A.; Isobe, K. *J. Organomet. Chem.* **1992**, *433*, 183.

(4) (a) Kang, J. W.; Maitlis, P. M. *J. Organomet. Chem.* **1971**, *30*, 127. (b) Nutton, A.; Bailey, P. M.; Maitlis, P. M. *J. Chem. Soc., Dalton Trans.* **1981**, 1997.

(5) Isobe, K.; Ozawa, Y.; Vázquez de Miguel, A.; Zhu, T.-W.; Zhao, K.-M.; Nishioka, T.; Ogura, T.; Kitagawa, T. *Angew. Chem., Int. Ed. Engl.* **1994**, *33*, 1882.

(6) Nishioka, T.; Kukushkin, V. Yu.; Isobe, K.; Vázquez de Miguel, A. *Inorg. Chem.* **1994**, *33*, 2501.

(7) Kaneko, Y.; Suzuki, T.; Isobe, K. *Organometallics* **1998**, *17*, 996.

(8) See the Supporting Information.

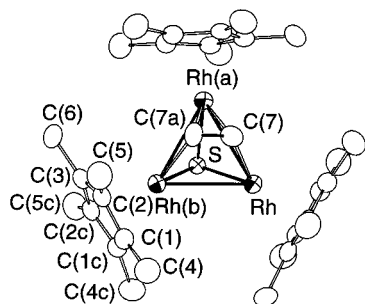
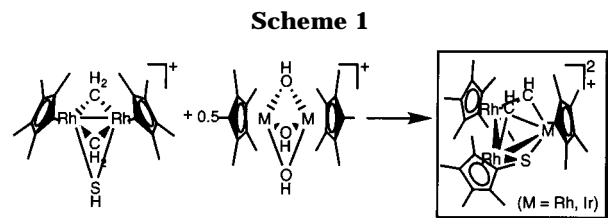


Figure 1. ORTEP diagram of the cationic moiety of **3b**.

complexes $[\text{IrRh}_2\text{Cp}^*_3(\mu_3\text{-}\eta^2\text{-}||\text{-C}_2\text{H}_2)(\mu_3\text{-S})]\text{X}_2$ (**4a**) and BF_4 (**4b**)⁸ were also prepared in a similar manner using $[\text{Ir}_2\text{Cp}^*_2(\mu_2\text{-OH})_3](\text{BPh}_4)$ (**2b**)^{4b} instead of $[\text{Rh}_2\text{Cp}^*_2(\mu_2\text{-OH})_3](\text{BPh}_4)$.

The structure of **3b** was confirmed by X-ray analysis⁹ together with FAB mass spectrometry and ¹H and ¹³C NMR spectroscopy.⁸ The cationic moiety of **3b** comprises an equilateral triangle of three rhodium atoms where one side of the triangle is capped by the triply bridging sulfido ligand and the other side by the acetylene ligand in a $\mu_3\text{-}\eta^2\text{-}||$ fashion, as shown in Figure 1. The Rh–Rh (2.8252(8) Å) and Rh–S (2.241(5) Å) bond distances are similar to those in $[\text{Rh}_3\text{Cp}^*_3(\mu_3\text{-S})_2](\text{BF}_4)_2$ (2.830(2) Å for Rh–Rh, 2.285(2) Å for Rh–S).¹⁰ Two carbon atoms of the C_2H_2 unit are disordered on the triangle (the standard deviation of the distance between them (1.12(5) Å) is fairly large),⁹ and the distance between them is somewhat shorter than that for the substituted $\mu_3\text{-}\eta^2\text{-}||\text{-C}_2\text{R}_2$ bonding mode.¹¹ The FAB mass and ¹³C NMR data⁸ also support the existence of the C_2H_2 unit; the ion-paired positive ion $\{[\text{Rh}_3\text{Cp}^*_3(\text{C}_2\text{H}_2)\text{S}]\text{BF}_4\}^+$ ($[\text{MBF}_4]^+$) and the singly ($[\text{M}]^+$) and doubly charged molecular ions ($[\text{M}]^{2+}$) were observed at m/z 859, 772, and 386, respectively; the nondecoupled ¹³C NMR signal at δ 144.6 with a double-doublet quartet has coupling constants of $^1J_{\text{C-H}} = 178$ Hz, $^2J_{\text{C-H}} = 2$ Hz, and $J_{\text{C-Rh}} = 9$ Hz due to an H–C–C–H skeleton.

This is the first example of acetylene formation from two $\mu_2\text{-CH}_2$ units. The hydroxide complex $[\text{Rh}_2\text{Cp}^*_2(\mu_2\text{-OH})_3](\text{BPh}_4)$ plays an important role in the abstraction of not only the proton of $\mu_2\text{-SH}$ but also that of $\mu_2\text{-CH}_2$ for the formation of the electronically saturated 48 e trinuclear cluster **3** with three Rh–Rh bonds. The fate of the hydroxide complex, however, is not yet clear. The intriguing proton abstraction from the $\mu_2\text{-CH}_2$ ligand in the analogous dirhodium complexes $[\text{Rh}_2\text{Cp}^*_2(\mu_2\text{-}$



$\text{CH}_2)(\text{CH}_3)_2$ and $[\text{Rh}_2\text{Cp}^*_2(\mu_2\text{-CH}_2)(\text{CO})\text{Ph}]^+$ has been proposed for some C–C bond formations under even nonbasic conditions.^{2c,12} The hydroxide complex gives one Rh unit to the Rh–Rh function for construction of the Rh_3 -triangle framework (Scheme 1). Our results may suggest that the $\mu\text{-CH}_2$ species, formed on the metal solid surfaces in the F–T and syngas reactions, has a chance of bringing about a similar reaction by interaction with M–OH functionalities on metal oxides to produce acetylene as an intermediary C_2 ¹³ hydrocarbon.

The dynamic property of **3b** in both solution and the solid state was studied by variable-temperature ¹H, ¹³C, and CP/MAS ¹³C NMR spectroscopy. The ¹H and ¹³C NMR spectra of the Cp* ligands in CD_3NO_2 shows a single signal at δ 2.00 for the CH_3 protons, at δ 107.9 for the ring carbons, and at δ 11.1 for the CH_3 carbons. The ¹⁰³Rh NMR signal resonates at δ 1218 as a singlet. The $\mu_3\text{-}\eta^2\text{-}||\text{-C}_2\text{H}_2$ ligand shows 1:3:3:1 quartet signals at δ 10.01 ($J_{\text{H-Rh}} = 3.3$ Hz) for the protons and at δ 144.6 ($J_{\text{C-Rh}} = 9$ Hz) for the carbons. These NMR results suggest that the three Rh moieties are magnetically equalized by the “windscreen-wiper motion”¹⁴ of the acetylene ligand, as observed in $[\text{Rh}_3\text{Cp}_3(\text{CO})(\text{PhC}\equiv\text{CPh})]$.¹⁵ A similar motion was also observed in **4b**, giving a 1:2:1 triplet signal for the $\mu_3\text{-}\eta^2\text{-}||\text{-C}_2\text{H}_2$ ligand in both the ¹H NMR and ¹³C NMR spectra. Even at -90 °C, the motion was not frozen (the spectral patterns and the line widths are the same as those at room temperature), in contrast with that of $[\text{Rh}_3\text{Cp}_3(\text{CO})(\text{PhC}\equiv\text{CPh})]$. In the variable-temperature CP/MAS ¹³C NMR spectrum for the solid state of **3b**, the acetylene and Cp* carbons exhibited a narrow single peak at room temperature, and the former peak was not broadened even at -120 °C, showing that the acetylene ligand is still mobile in the solid state at low temperature.⁸ This suggests that the cavity constructed by the three Cp* ligands and the Rh triangle provides enough space for the motion of the acetylene ligand regardless of the state (solution or solid) of **3b**, and its activation energy is too small to freeze the motion. An additional motional process was also found: at -120 °C each signal of the ring and the methyl carbons of the Cp* ligand splits into four peaks with a 1:1:1:2 intensity ratio (Figure 2). The methyl groups and the ring carbons within the Cp* ligand are not equivalent,

(9) The two carbon atoms of the C_2H_2 ligand are disordered in three places on each side of the triangle of Rh_3 (the S atom is also disordered), and this disorder puts two carbons with $1/6$ occupancy close enough that their individual positions cannot be located. Hence, the ellipsoids of acetylene carbon atoms are distorted as shown in Figure 1, and the positions of the carbon atoms used for the calculation for the C–C bond distance are not precisely determined. In addition, the standard deviation of the C–C alkyne bond distance is large, as described below and in p 3. Crystal data for $[\text{Rh}_3(\text{Cp}^*_3(\mu_3\text{-}\eta^2\text{-}||\text{-C}_2\text{H}_2)(\mu_3\text{-S}))](\text{BF}_4)_2 \cdot \text{C}_{32}\text{H}_{47}\text{B}_2\text{F}_8\text{Rh}_3\text{S}$ (fw = 952.13); hexagonal, space group $P6_3/m$ (No. 176), $a = 11.430(1)$ Å, $c = 15.743(2)$ Å, $V = 1781.2(4)$ Å³, $Z = 2$, $D_{\text{calcd}} = 1.764$ g cm⁻³, $D_{\text{obsd}} = 1.75$ g cm⁻³, $\mu(\text{Mo K}\alpha) = 1.47$ mm⁻¹, crystal size $0.36 \times 0.11 \times 0.11$ mm. The full-matrix refinements of 105 least-squares parameters and 1054 reflections converged at R (R_w) = 0.038 (0.045). Selected bond lengths (Å) and angles (deg): Rh–Rh(a), 2.8252(8); Rh–S, 2.241(5); Rh–C(7), 2.16(2); Rh–C(7a), 2.19(2); C(7)–C(7a), 1.12(5); Rh–S–Rh(a), 78.1(2); Rh–C(7)–Rh(b), 80.9(7).

(10) Nishioka, T.; Isobe, K. *Chem. Lett.* **1994**, 1661.

(11) Sappa, E.; Tiripicchio, A.; Braunstein, P. *Chem. Rev.* **1983**, *83*, 203.

(12) Saez, I. M.; Meanwell, N. J.; Nutton, A.; Isobe, K.; Vázquez de Miguel, A.; Bruce, D. W.; Okeya, S.; Andrews, D. G.; Ashton, P. R.; Johnstone, I. R.; Maitlis, P. M. *J. Chem. Soc., Dalton Trans.* **1986**, 1565.

(13) Maitlis, P. M.; Saez, I. M.; Meanwell, N. J.; Isobe, K.; Nutton, A.; Vázquez de Miguel, A.; Bruce, D. W.; Okeya, S.; Andrews, D. G.; Ashton, P. R.; Johnstone, I. R. *New J. Chem.* **1989**, *13*, 419 and references therein.

(14) Busetto, L.; Green, M.; Hessner, B.; Howard, J. A. K.; Jeffery, J. C.; Stone, F. G. A. *J. Chem. Soc., Dalton Trans.* **1983**, 519.

(15) Todd, L. J.; Wilkinson, J. R.; Rausch, M. D.; Gardner, S. A.; Dickson, R. S. *J. Organomet. Chem.* **1975**, *101*, 133.

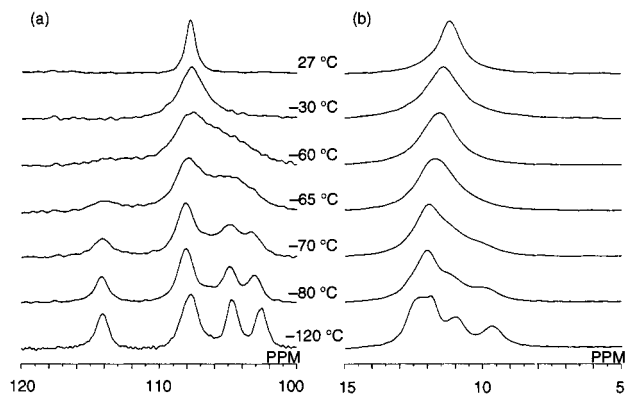


Figure 2. Temperature dependence of the cyclopentadienyl ring (a) and methyl (b) signals in solid-state CP/MAS ^{13}C NMR spectra of **3b**.

due to the cessation of the jumping motion of the Cp^* ligand, but the three Cp^* ligands in **3b** are still equalized by the windscreen-wiper motion of the acetylene ligand. When the temperature was elevated, these peaks exhibited signs of exchange averaging in response to the reorientation that occurs due to the jumping

motion. From the coalescence temperatures ($-65\text{ }^\circ\text{C}$ for methyl and $-30\text{ }^\circ\text{C}$ for the ring) the activation energy for the Cp^* reorientation was estimated to be 18 kJ mol^{-1} , which is higher than the 13.5 kJ mol^{-1} value reported for decamethylferrocene.¹⁶

We have isolated the two-electron-reduced (50-electron) species of **3b**,¹⁷ which shows a much slower dynamic motion than **3b**, and are now elucidating various factors to determine the rate of motion.

Supporting Information Available: Text giving experimental procedures and characterization data for **3** and **4**, tables giving full details of the crystal structure analysis for **3b**, and a figure giving variable-temperature CP/MAS ^{13}C NMR spectra for $[\text{Rh}_3\text{Cp}^*_3(\mu_3\text{-}\eta^2\text{-I-C}_2\text{H}_2)(\mu_3\text{-S})](\text{BF}_4)_2$ (9 pages). Ordering information is given on any masthead page.

OM970796J

(16) (a) Wemmer, D. E.; Ruben, D. J.; Pines, A. *J. Am. Chem. Soc.* **1981**, *103*, 28. (b) Braga, D. *Chem. Rev.* **1992**, *92*, 633.

(17) The half-wave potentials ($E_{1/2}$ vs Fc^+/Fc) of three reversible reduction processes for **3b** in MeCN at a scan rate of 100 mV/s are as follows: $2^+ \rightarrow 1^+$, $E_{1/2} = -0.94\text{ V}$; $1^+ \rightarrow 0$, $E_{1/2} = -1.08\text{ V}$; $0 \rightarrow 1^-$, $E_{1/2} = -2.61\text{ V}$. An irreversible oxidation wave was also observed at 1.26 V .